ELSEVIER

Materials Science and Engineering A 467 (2007) 125–131

MATERIALS SCIENCE & ENGINEERING A

www.elsevier.com/locate/msea

Influence of firing temperature on interface adhesion between screen-printed Ag film and $BaTiO_3$ substrate

Chao-Yu Lee [a,b,*], Michel Dupeux [b], Wei-Hsing Tuan [a]

[a] *Department of Materials Science and Engineering, National Taiwan University, Taipei 106, Taiwan*

[b] *Laboratoire de Thermodynamique et Physico-Chimie Métallurgiques (LTPCM), Universite Joseph Fourier, Grenoble, France*

Received 9 August 2006; received in revised form 19 February 2007; accepted 21 February 2007

Abstract

Interfaces between porous metal and ceramic are commonly used in many advanced engineering components. The adhesion strength between a porous silver coating and pure barium titanate has been determined here using a blister test. The porous Ag layer was made by screen printing and sintering on a flat dense barium titanate surface. Firing temperature influences the porosity of the silver film and Ag/$BaTiO_3$ interface strength. A simple graphic procedure was used to subtract the effect of the generalized plastic yielding in the Ag membrane from the total strain energy produced by the pressure application. The average value of the critical interface crack propagation energy G_{ci} at the porous Ag/$BaTiO_3$ interface ranges between 4.5 and 6.6 J/m^2 while the porosity decreases from 11% to 7%. The observed trend of interfacial fracture energy can offer insights into the interfacial fracture mechanisms between porous metal films and ceramic substrates.
© 2007 Elsevier B.V. All rights reserved.

Keywords: Adhesion; Ag/barium titanate interface; Porosity; Interfacial crack propagation energy

1. Introduction

Metal–ceramic interfaces play an important role in many applications, such as electronic packages, ceramic brazing, wear resistant coatings, thermal barrier coatings or micro-electromechanical systems. The metal–ceramic interfacial strength is an important parameter for all applications since it fully governs the integrity of the device of interest. Among many techniques, screen printing and sintering is a low-cost method to make a metal film bonded to a ceramic substrate. It is generally used to fabricate multilayer ceramic capacitors (MLCC), sensors, device structure, etc. This technique produces a porous metal layer; the porosity of the metal film depends on the various chemical and physical characteristics of the metal paste and on its firing temperature.

Many different methods have been proposed to measure the adhesion strength of metal-oxide interface, either as bulk bi-material or as film/substrate systems [1,2]. The blister test is one of the few techniques which can deliver quantitative and meaningful estimation on interfacial strength. Thanks to a stable interfacial crack growth under a constant and well-known mode mixity for film/substrate systems, it allows reliable quantitative interfacial fracture energy measurements [3,4]. For this test, a rigid film/substrate specimen has to be prepared with a free-standing film membrane covering a hole located at the center of the specimen. During a first step of the experiment, the free-standing membrane is pressurized by liquid injection through the hole in the substrate, keeping the contour of the initial window. This "bulge" step is reported as an increasing curve when plotting the pressure p versus the membrane maximum deflection h. The elastic bulging of the membranes can be analyzed using various models to describe their mechanical equilibrium and geometry [5–10].

When the pressure is high enough and the liquid injection is continued, the film starts to debond along the edges of the window. The outline of the membrane changes from its initial shape and its volume increases rapidly, thus causing a decrease of the fluid pressure and a visible change of regime on the p versus h curve. By applying the energy balance between the increase of the fluid energy W_{fluid} and the membrane strain energy W_{strain}, the differential of the crack propagation energy can be written as

$$G_{ci} 2\pi a \mathrm{d}a = \frac{\partial W_{fluid}}{\partial a}\mathrm{d}a - \frac{\partial W_{strain}}{\partial a}\mathrm{d}a \quad (1)$$

* Corresponding author at: Department of Materials Science and Engineering, National Taiwan University, Taipei 106, Taiwan. Tel.: +886 2 33662679.
E-mail address: d92527006@ntu.edu.tw (C.-Y. Lee).

0921-5093/$ – see front matter © 2007 Elsevier B.V. All rights reserved.
doi:10.1016/j.msea.2007.02.077

where da is the elemental crack growth and G_{ci} is the fracture energy per unit area. Estimates each term of Eq. (1) shows that the p versus h curve should then follow a decreasing hyperbolic law:

$$Cph = G_{ci} \tag{2}$$

where C is a numerical dimensionless constant between 0.618 and 0.516 according to the residual stress value in the film [11,12].

In the present study, the blister test was used to measure the adhesion strength between screen printed silver films and barium titanate substrates.

2. Experimental procedures

2.1. Materials and specimens

A barium titanate powder (Product No. 52909, Ferro Co., USA) was used in the present study. The purity of the $BaTiO_3$ powder was higher than 99.6% and the average particle size was 1.1 μm. Discs of $BaTiO_3$ (25 mm in diameter and 2.5 mm in thickness) were prepared by die-pressing at 50 MPa. The discs were first pre-fired at 1100 °C for 1 h to obtain a handling strength. A hole with 3 mm diameter was then machined into the center of the pre-fired discs by using a steel drill. The discs were then sintered at 1350 °C for 2 h. The diameter of the hole shrank to 2.1 mm after firing. The relative density of $BaTiO_3$ is then >98%. Finally the discs were ground with fine SiC particles to achieve a flat smooth surface. The final substrate surface roughness R_a was about 0.2 μm, as measured with a profilometer.

A silver paste composing of silver particles, binder and a small amount of glass particles was prepared for screen printing. A silver powder (Ag C200ED, Ferro Co., USA) with average particle size of 1.1 μm was used. The silver powder/glass frit ratio was 98.75/1.25 in weight. The powder/organic vehicle ratio was 80/20 in weight. All were mixed and milled with the help of a media mill. Screen-printing was used to apply the Ag paste onto the flat surface of the $BaTiO_3$ discs. Round adhesive tape patches 3 mm in diameter were applied on a $BaTiO_3$ plate. The Ag layer was screen printed over the whole surface, and then the $BaTiO_3$ plate with Ag layer and adhesive patches was fired at 500 °C for 1 h to remove the adhesive tape. Therefore, we could obtain several pre-fired silver membranes with 10 μm thickness and 3 mm diameter, which were used to cover the central hole of the discs as free-standing Ag membranes. The discs including these free-standing membranes over the holes were then screen printed with Ag electrode for several times until the desired thickness of Ag layer is achieved and fired at 600, 700, 800 or 850 °C for 1 h.

2.2. Experimental apparatus

The apparatus used for the blister test consisted of a specimen holder and pressurizing stage, and an optical fringe projection profilometer. A commercial software (HOLO-3: Fringe Analysis®, France) was used to analyze the results in terms of blister radius and deflection at various steps of each test. The complete setup of facilities has been described in more details in previous papers [13,14].

For each firing temperature, some of the specimens were cold mounted and cut transversally and then prepared by standard metallographic techniques. The cross-section microstructures were observed by scanning electron microscopy. Quantitative analysis of digitalized images (ImageJ 1.34s) was used to determine the porosity of the screen printed silver films.

2.3. Analysis of blister test results

For many film-on-substrate systems, it is usually assumed that the top film deforms elastically. Because of its thickness, our porous silver layer has a low yield stress and tends to deform plastically. Then the strain energy dissipated during the blister test is composed of the work of elastic deformation and the work of plastic deformation. They have to be separated for adhesion measurement, since only the elastic strain energy is reversible and can be released from the pressurized membrane to cause the interface crack propagation.

Experimentally, when conducting the blister test, a hydraulic pressure is applied to make the metal layer blister and separate from its substrate. Then the pressure is released progressively and the p versus h curve generally falls down along a linear path and shows a residual deflection h_p, proving that the film has been plastically deformed. After the first pressurization and debonding, as long as the system is stable we can re-inject liquid to make blistering occur again and then release the pressure again. Therefore, each repeated pressurization can be used to determine the adhesion energy of the interface by fitting a hyperbolic curve to the debonding threshold points according to Eq. (2). At each pressurization, since we record successive 3D contours of the complete blister, we can check the diameter values to determine as accurately as possible the point when the blister begins to grow and the interfacial crack begins to propagate. We defined this point as the critical point to be used for G_c determination. In many cases, we can obtain several debonding points on one specimen till the metal layer is broken or totally de-bonded. Since the Ag membrane behaviour is dominated by residual stress (due to thermal contraction mismatch between metal and ceramic after firing), we used $C = 0.516$ in Eq. (2) for result analysis in this study [4,11].

For each re-pressurization, since the film has deformed plastically after previous pressurization, the volume underneath the new free-standing membrane can be related to its previous plastic residual deflection height h_p. The total strain energy of the pressurized film should then be changed to

$$U_{strain} = \int_0^{h_p+h} p(h)\,dV = \int_0^{h_p} p(h)\,dV + \int_{h_p}^{h} p(h)\,dV \tag{3}$$

The strain energy contributed by the plastic deformation should be extracted from the total apparent strain energy, to work out the elastic energy release rate which causes crack

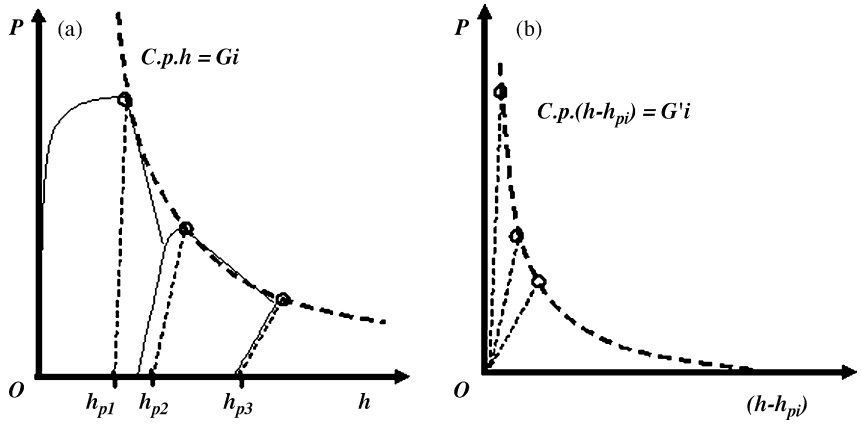

Fig. 1. Schematic of the principle of correction for the effect of the generalized plasticity of the silver membrane on the interfacial debonding energy.

propagation. A very simple way to correct this plastic bulging of the membrane is to subtract the corresponding residual permanent deflection h_{pi} for each quasi-linear inflation-deflation elastic curve at a critical point for a given specimen, as illustrated on Fig. 1. The critical debonding points then correspond to much smaller values of corrected deflection $(h - h_{pi})$ just as if the membrane had remained elastic throughout the test, and they are located on such hyperbola $Cp(h - h_{pi}) = G_i'$ with much smaller and more reliable values of debonding energy.

For example, Fig. 2 shows the blister equation fit to the experimental data at the de-bonding point for a specimen with a silver layer fired at 850 °C. The uncorrected crack propagation energy was acquired as 11 J/m^2, while the height being corrected as $h = h_{exp} - h_{pla}$, the result diminished to 4.5 J/m^2. Thanks to this very simple procedure, we can subtract the effect of the generalized plastic yielding in the Ag membrane from the total strain energy produced by the pressure application.

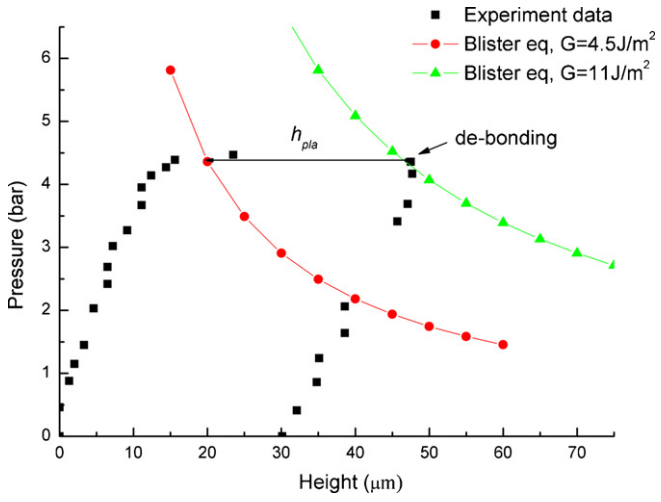

Fig. 2. Illustration of blister equation fit to experimental data for a specimen fired at 850 °C. The uncorrected value $G = 11$ J/m^2 is adjusted on the experimental debonding point. The corrected value $G' = 4.5$ J/m^2 is adjusted on the corrected debonding height, according to the schematic of Fig. 1.

3. Results

3.1. Microstructure observations

Fig. 3 shows an SEM image of a cross-section of the specimen after sintering. The Ag/$BaTiO_3$ interface appears to be relatively smooth and abrupt at the magnification we used. The thickness of the silver layer has been changed between 55 and 130 μm. It was been measured after sintering by micrometer screw gauge, with reference to the initial substrate thickness. For each substrate and substrate with film, five points were measured and the average was taken as thickness.

For our purpose of adhesion measurement, the porosity within the Ag/$BaTiO_3$ interface is very likely to have a strong influence on the interfacial crack propagation energy, but it is very difficult to determine experimentally from optical or SEM observations. In the following, we take the interface porosity (defined as the ratio of the non-contacting area to the total interface area) from the internal porosity in the bulk of the silver layer.

Fig. 3(a) shows the Ag layer fired at 600 °C for 1 h. The pores within the sintered metal are interconnected and the average porosity is 11%. Fig. 3(b) shows the silver film fired at 700 °C. It can be observed that most of the pores are no longer interconnected and the average porosity is 10%. When the firing temperature was raised to 800 °C (Fig. 3(c)), the average porosity of Ag film became 8%. The shrinkage rate of Ag film from 700 to 800 °C is higher than that between 600 and 700 °C. Fig. 3(d) shows the silver film fired at 850 °C and the average porosity in the silver film is 7%. The size of the pore within the Ag film is increased after the treatment at 850 °C, though their amount is more or less the same as that in the film fired at 800 °C.

3.2. Results of blister test

The resulting critical energy release rates G_{ci} of the $BaTiO_3$/Ag interfaces for each Ag paste sintering temperature are listed in Table 1. As explained before, these values are corrected by removing the influence of generalized plastic deformation of the membrane, but they still include the contri-

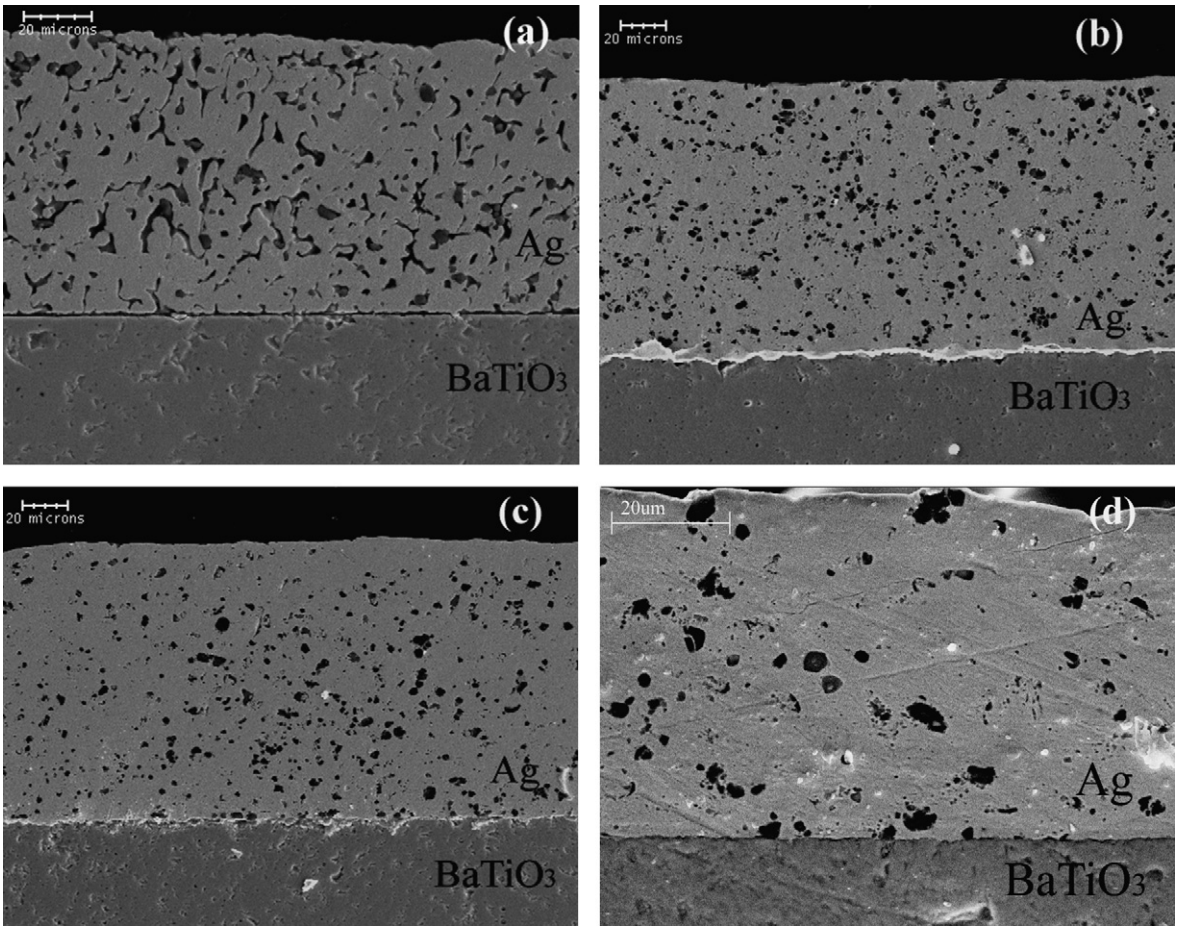

Fig. 3. Cross-section views of Ag/$BaTiO_3$ interfaces. Ag films were fired at (a) 600 °C, (b) 700 °C, (c) 800 °C and (d) 850 °C.

bution of the confined plasticity which is likely to occur at the crack tip during the propagation of the interfacial crack, just like cohesive crack propagation energy in any ductile homogeneous metal. The values of G_{ci} for specimens which are fired at 600 °C, vary from 3.5 to 5.5 J/m^2. The values of G_{ci} for interfaces fired at 700 °C vary from 3 to 6 J/m^2, which is close to the result of 600 °C. The inter-particle contact area for sintered powders increases while firing temperature increased from 600 to 700 °C (Fig. 3(a) and (b)). It seems that the subsequent decrease of porosity does not affect much the interface strength at this stage. The values of G_{ci} fired at 800 °C vary from 3.5 to 8 J/m^2, with an overall average value around 5.8 J/m^2. At 850 °C the critical energy release rate of interface cracks ranges from 4.5 to 9 J/m^2.

4. Discussion

Table 1 also shows the thicknesses of specimens fired at 600, 700 and 800 °C. In the same firing condition, the influence of the film thickness on interface strength seems to be smaller than the experimental dispersion of the energy values. Therefore, it will not be considered in the following discussion.

The relation between average G_{ci} and sintering temperature is shown in Fig. 4. The critical energy release rate of interface cracks increases when the firing temperature increases, especially in the range from 700 to 800 °C. This may be due to the changes in the pore volume through the metal membrane and similarly along the interface. Indeed, some un-bonded pore-like defects are visible at the interface, for all firing temperatures (Fig. 3), which are due to influence the adhesion strength of Ag/$BaTiO_3$ interface.

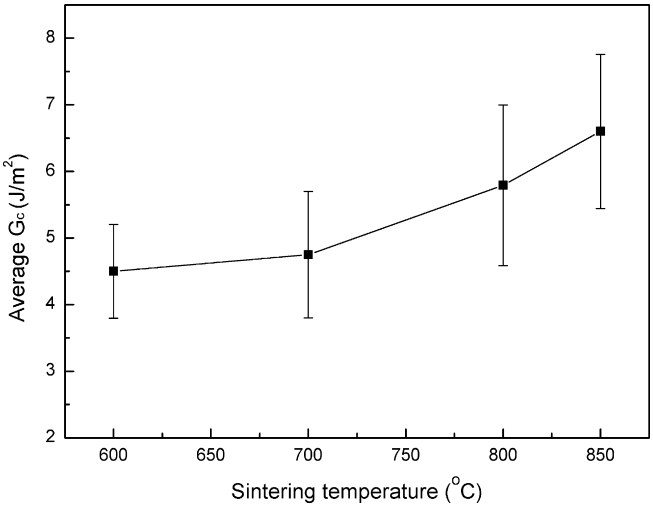

Fig. 4. Average fracture energy of interface versus sintering temperature of silver membrane.

Table 1
The critical interfacial energy release rates G_{ci} of Ag/$BaTiO_3$ interfaces

Firing temperature (°C)	G_c of successive pressurizations (J/m^2)	Sample no.								Porosity (%)
		1	2	3	4	5	6	7	Average	
600	G_{c1}	5	5	5.5	3.5	4				
	G_{c2}	4								
	Average	4.5	5	5.5	3.5	4			4.5 ± 0.71	11
	Thickness (μm) ± 10	108	75	125	68	109				
700	G_{c1}	5.5	5	5	3	5	6			
	G_{c2}			3	4	5	5			
	Average	5.5	5	4	3.5	5	5.5		4.75 ± 0.95	10
	Thickness (μm) ± 10	73	84	67	97	86	114			
800	G_{c1}	5	6	8	6	5	6			
	G_{c2}	5		8	5	5				
	G_{c3}	3.5			5					
	G_{c4}				5					
	Average	4.5	6	8	5.25	5	6		5.8 ± 1.21	8
	Thickness (μm) ± 10	95	128	83	74	71	117			
850	G_{c1}	6	8	6	4.5	6	7	6		
	G_{c2}		9	7	7		8	7		
	G_{c3}			6.5	7		6			
	G_{c4}				5					
	G_{c5}				5					
	Average	6	8.5	6.5	5.7	6	7	6.5	6.60 ± 1.16	7

Fig. 5 shows the critical energy release rate G_{ci} of Ag/$BaTiO_3$ interfaces versus the porosity of the Ag film. The silver paste used in this study was named as G-1. Within the range of membrane porosity from 11% to 7%, the G_{ci} of the interface between porous silver membrane and $BaTiO_3$ substrate is almost a linear function of the porosity of the membrane. It is obvious that smaller contact areas across the metal/ceramic interface will reduce the interface strength. But for a given interface porosity, the size and shape of interface cavities must also play a role. Indeed, large round-shape cavities might blunt interface cracks and rather tend to prevent their propagation, while small fine-dispersed elongated cavities should cause high interface embrittlement. Some authors have reported finite element analysis simulation of a crack growth along the interface between a porous ductile material and a rigid substrate [15,16]. But very few experimental data for interfacial crack propagation between porous metal film and ceramic substrate are available in literature [17] – maybe because of the difficulty to characterize the interface porosity [18], as mentioned before – and even less under the form of quantitative adhesion measurement to be compared to our results. Thus the relation between the critical energy release rate of interface cracks and interface contact area is still not clear now.

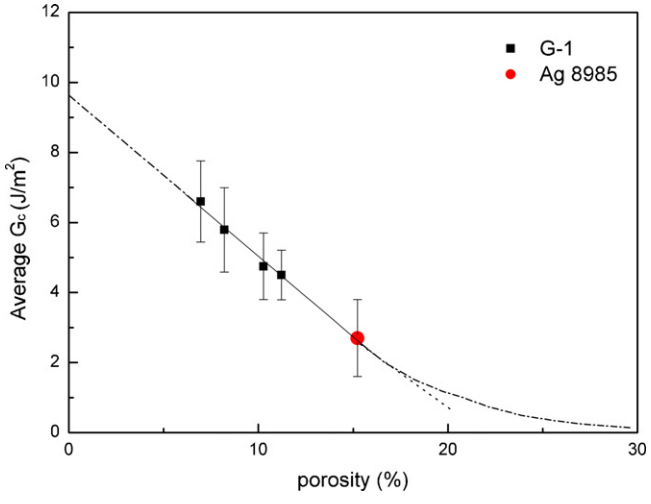

Fig. 5. Average fracture energy of interface versus average porosity of silver membrane. (■) Present work; (●) previous report [14].

Comparing the results at the same firing temperature we had reported previously [14], where the values of G_{ci} vary from 1.3 to 4.2 J/m^2 for Ag/$BaTiO_3$ interfaces, the results in the present work are much higher. The major differences between both studies are Ag powder particle size and chemical composition of Ag pastes. Both factors are likely to change the porosity of the film after firing and altogether the value of the thermodynamical interfacial work of adhesion itself. In Fig. 5, the values of the present work are plotted together with the previously reported adhesion strength of other silver paste (Ag 8985) to barium titanate [14], with the porosity measured using the same procedure. Both silver layer pastes contained some glass mixed with organic solvent and binder. From Fig. 5 we can observe that the chemical composition of the silver paste did not seem to influence much on interface adhesion. Contact area seems to play a more important role in the interface adhesion, since the same linear dependence of G_{ci} on porosity appears to be valid for both Ag pastes.

Such a linear relationship is actually the simplest assumption which may be made to account for the dependence of crack propagation energy on interfacial porosity. Extrapolating the linear fit of Fig. 5 to a zero porosity value would lead to crack propagation energy about 10 J/m^2 for a full-contact Ag/$BaTiO_3$ interface, which is a rather reasonable value for metal/ceramic interface adhesion [2]. On the reverse, a linear extrapolation of our results to higher porosity rates would lead to null crack propagation energy far before 100% porosity, which is not physically acceptable. So, another extrapolation law should apply for porosity higher than about 15%, compatible with complete loss of adhesion only for 100% interfacial porosity. Another possible cause for this discrepancy is that our assumption taking the interfacial porosity equal to the bulk porosity in Ag is grossly wrong, which is difficult to verify, but looks unlikely as close as we could observe our metal/ceramic interfaces. More experiments with better accuracy and a wider range of Ag membrane porosity will be necessary to clear these points.

The main contribution to the uncertainty of our results may be attributed to the difficulty in determining the accurate critical de-bonding points and subtracting the plastic strain contribution. Even taking this incertitude into account, our crack propagation energy values are higher than the usual estimates of the thermodynamical work of adhesion of metal/ceramic interfaces alone, around 1 J/m^2.

Indeed, the basic thermodynamic property of an interface between materials A and B is its free energy per unit area γ_{AB}. In experimental measurement, a different quantity can be determined: the true work of adhesion W_a (or so-called Dupré energy) which is the amount of energy required to create free surfaces from bonded materials:

$$W_a = \gamma_A + \gamma_B - \gamma_{AB} \tag{4}$$

where γ_A and γ_B are the surface energies of the two materials, respectively. The true work of adhesion is the intrinsic property that depends on the type of the bonds at the interface and the level of contamination on the initial surfaces. The metal–ceramic system of interest here cannot be considered as a very reactive one. The chemical reaction at interface is $2Ag + 1/2O_2 \rightarrow Ag_2O$ and Ag_2O will be promptly decomposed [19]. This means that no reaction layer exists at Ag/$BaTiO_3$ interface and Ag does not diffuse into the $BaTiO_3$.

The true work of adhesion can be determined by contact angle measurements with the sessile drop technique, through the Young–Dupré equation, which describes W_a as the function of the contact angle θ:

$$W_a = \gamma_A + \gamma_B - \gamma_{AB} = \gamma_B(1 + \cos\theta). \tag{5}$$

In the specific case of Ag/$BaTiO_3$ interfaces, the contact angle in the Ag/$BaTiO_3$ is about 90 [19] while the surface energy of silver is 1.25 J/m^2 [20]. Thus, W_a of Ag/$BaTiO_3$ interface can be estimated to be around 1.25 J/m^2. But the practical crack propagation energy G_{ci} is always higher than W_a. This difference, which has been extensively discussed in literature [1,21,22], is usually explained by the various contributions of three multiplicative factors:

- The first one is the non-equilibrium thermodynamic state of the newly created fracture surfaces, and is estimated between 1 and 10.
- The second one is the effect of interface roughness, which causes the true contact area to be larger than its projected measurable value. This factor is generally only slightly larger than 1.
- The third factor is the energy dissipation through confined plastic deformation of materials at the interfacial crack tip.

Therefore, the G_{ci} usually exceeds W_a by two or even three orders of magnitude and reach values as high as hundreds of J/m^2 [23]. In our case, the first factor is certainly partly responsible for the difference between $W_a \cong 1.25$ J/m^2 and $G_{ci} \cong 10$ J/m^2 for a full-contact Ag/$BaTiO_3$ interface. But, even if we managed to subtract the energy contribution of generalized plastic deformation of the silver membrane, it is very likely that an important amount of confined plastic flow occurs at the crack tip on the side of the silver component, which is known as a very ductile material. This contribution of confined plasticity cannot be subtracted, and is actually inherent in the crack propagation phenomenon, and thus contributes to the mechanical strength of the interface.

5. Conclusion

Specimens with porous Ag layer, fabricated at four sintering temperatures to produce different porosity, covering a dense $BaTiO_3$ substrate have been prepared with a special geometry appropriate for blister testing. The blister test technique allows estimation of interfacial adhesion strength through determination of the interfacial crack propagation energy. A simple method is proposed to overcome experimental difficulties such as generalized plastic straining of the porous metal layer. With this procedure, the critical crack propagation energy of the interface between the Ag layers with various porosities on $BaTiO_3$ has been measured. The average value increases from 4.5 to 6.6 J/m^2 while the porosity decreases from 11% to 7%. So, the technique which has been set up here is one of the few which is able to provide quantitative reliable values for metal/ceramic practical adhesion energies. It has proved to be applicable to the Ag/$BaTiO_3$ system, which is of interest for multi-layer ceramic capacitors, and it is expected to be useful for more detailed exploration of the effect of various parameters governing metal–ceramic interfacial adhesion. Experimental attempts are presently made to cross-check its results with other adhesion measurement techniques, like cross-sectional indentation, on the same metal–ceramic interfaces.

Acknowledgements

The present study was supported by the National Science Council, Taiwan, through the contract numbers of NSC94-2216-E-002-008 and NSC94-2218-E-002-043 and Centre National de la Recherche Scientifique, France. The practical and financial help from the Institut Français de Taipei to C.Y. Lee and to the

student exchange program between National Taiwan University, Taipei, and Université Joseph Fourier, Grenoble, is highly appreciated.

References

[1] F. Ernst, Mater. Sci. Eng. R 14 (1995) 97–156.
[2] A.A. Volinsky, N.R. Moody, W.W. Gerberich, Acta Mater. 50 (2002) 441–466.
[3] A. Bosseboeuf, M. Dupeux, M. Boutry, T. Bourouina, in: H. Oettel, S. Hogmark, J. von Stebut (Eds.), Proceedings of the International Workshop on "Mechanical behaviour of P.V.D. Coated Materials", Holzau/Erzgebirge (Allemagne), Technische Universität Bergakademie Freiberg, October 13–17, 1998, pp. 169–181.
[4] M. Dupeux, A. Bosseboeuf, in: A. Bellosi, et al. (Eds.), Interfacial Science in Ceramic Joining, Kluwer Acad. Publ., Boston, 1998, pp. 319–327.
[5] R.J. Hohlfelder, J.J. Vlassak, W.D. Nix, H. Luo, C.E.D. Chidsey, Mater. Res. Soc. Symp. Proc. 356 (1995) 585–590.
[6] O. Tabata, K. Kawahata, S. Sugiyama, I. Igarashi, Sens. Actuators 20 (1989) 135–141.
[7] M.K. Small, J.J. Vlassak, S.F. Powell, B.J. Daniels, W.D. Nix, Mater. Res. Soc. Symp. Proc. 308 (1993) 159–164.
[8] V.M. Paviot, J.J. Vlassak, W.D. Nix, Mater. Res. Soc. Symp. Proc. 356 (1995) 579–584.
[9] E. Bonnotte, P. Delobelle, L. Bornier, B. Trollard, G. Tribillon, J. Phys. III 5 (1995) 953–983.
[10] D. Maier-Schneider, J. Maibach, E. Obermeier, J. Microelectromech. Syst. 4 (4) (1995) 238–241.
[11] R.J. Hohlfelder, H. Luo, J.J. Vlassak, C.E.D. Chidsey, W.D. Nix, Mater. Res. Soc. Symp. Proc. 436 (1997) 115–120.
[12] J. Sizemore, D.A. Stevenson, J. Stringer, Mater. Res. Soc. Symp. Proc. 308 (1993) 165–170.
[13] J. Mougin, M. Dupeux, A. Galerie, L. Antoni, Mater. Sci. Technol. 18 (2002) 1217–1220.
[14] C.-Y. Lee, M. Dupeux, W.-H. Tuan, Scripta Mater. 54 (2006) 453–457.
[15] E. Radi, M.C. Porcu, Int. J. Solids Struct. 38 (2001) 8235–8258.
[16] E. Radi, D. Bigoni, J. Mech. Phys. Solids 44 (1996) 1475–1508.
[17] K. Suganuma, in: A. Bellosi, et al. (Eds.), Interfacial Science in Ceramic Joining, Kluwer Acad. Publ., Boston, 1998, pp. 249–265.
[18] M.V. Oliveria, L.C. Pereira, C.A.A. Cairo, Mater. Res. 5 (2002) 269–273.
[19] S. Sugihara, K. Okazaki, Application of Ferroelectrics, Proceedings of the 7th IEEE International Symposium, 1990, pp. 432–434.
[20] H.L. Skriver, N.M. Rosengaard, Phys. Rev. B 46 (11) (1992) 7157–7168.
[21] H.C. Cao, A.G. Evans, Mech. Mater. 7 (1989) 295–304.
[22] A.G. Evans, M. Rühle, B.J. Dagleish, P.G. Charalambides, Met. Trans. A 21A (1990) 2419–2429.
[23] E. Felder, E. Darque-Ceretti, Adhésion et Adhérence, CNRS Edt, Paris, 2003.